

# Characterization of an External Combustion Dynamic Micro Heat Engine

L. W. Weiss, K. E. McNeil, D.F. Bahr, C.D. Richards and R.F. Richards  
PowerMEMS Conference  
School of Mechanical and Materials Engineering  
Washington State University  
Tel (509) 335-8157, Fax (509) 335-4662, E-mail richards@mme.wsu.edu  
Pullman, Washington 99164-2920, U.S.A.

## Abstract

Progress toward the realization of an external combustion dynamic micro heat engine is documented. First, previous work on three engine components: the piezoelectric membrane generator, the thermal switch and the wicking evaporator are summarized. Second, the internal irreversibility of the engine is quantified with measurements of viscous dissipation. Finally, the integration of a thermal switch with an engine is described. The thermal switch is shown to be an effective means to control heat transfer into the engine from a continuous heat source and out of the engine to a continuous heat sink. The use of the thermal switch is shown to enable engine cycle speeds up to 100 Hz.

*Keywords: dynamic micro heat engine*

## 1. INTRODUCTION

On the macro-scale, dynamic heat engines have achieved great success as power sources, much greater than either fuel cells or static heat engines. This success is in large part because dynamic heat engines are more fuel flexible than fuel cells and have achieved higher conversion efficiencies than static heat engines. This success has motivated a variety of designs for micro-scale dynamic heat engines. These include a gas turbine (Brayton cycle) engine [1], and a micro rotary internal combustion (Otto cycle) engine [2]. Both of these dynamic heat engines are internal combustion engines.

Work in our lab has focused on an external combustion dynamic micro heat engine designed to produce electrical power by employing a three-part strategy. First, thermal power is periodically conducted into the engine from an external heat source via a thermal switch. Second, thermal power is converted to mechanical power through the expansion and compression of a two-phase working fluid and the consequent oscillation of a flexible membrane. Third, mechanical power is converted into electrical power through the periodic straining of a thin-film piezoelectric generator fabricated on the membrane.

As shown in Fig. 1, an individual engine consists of a cavity filled with a saturated, two-phase working fluid, bounded on the top and bottom by thin membranes. The bottom membrane acts as the evaporator. A capillary wick fabricated on the bottom membrane controls the layer of liquid-phase working fluid on the

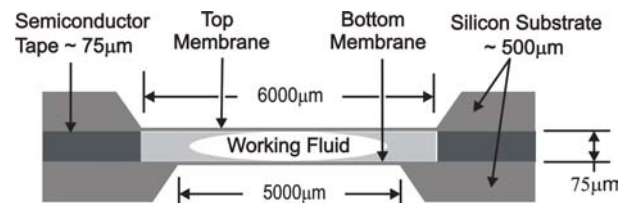


Figure 1. Engine Cross-Section

evaporator. The top membrane of the cavity is a thin film piezoelectric membrane generator.

A thermal switch is used to periodically conduct heat in or out of the two-phase working fluid, through the thin membranes capping the cavity at top and bottom. As heat is conducted first into and then out of the working fluid, the quality and volume of the saturated mixture first increases and then decreases. As a consequence, the upper membrane flexes in and out straining the piezoelectric thin film deposited on it. In this way, the piezoelectric membrane acts alternately as an expander and as a compressor during the engine cycle. The useful output of a unit cell engine is the electrical power generated by the piezoelectric membrane as it is strained during expansion of the two-phase working fluid.

Past work in our group has focused on developing components for the engine, including the piezoelectric membrane generator that transduces mechanical power into electrical power, the thermal switch responsible for controlling heat transfer in and out of the engine, and the wicking evaporator that controls the flow and position of liquid-phase working fluid in the engine.

Theoretical work on the piezoelectric generator, validated by experimental measurements, has shown how generator efficiency depends on quality factor  $Q$  and piezoelectric coupling coefficient  $k^2$ . Membrane generators with conversion efficiencies (mechanical to electrical) of 34% have been fabricated and tested. Modeling work indicates that generator efficiencies of 70% are possible through control of membrane boundary conditions and residual stress [3].

Work on the thermal switch has focused on realizing a switch design in which an array of liquid-metal micro-droplets deposited on a silicon substrate makes and breaks contact with a second silicon membrane. Experimental heat transfer measurements made on a prototype thermal switch using a guard-heated calorimeter have demonstrated thermal resistances of less than 1 °C/W for the “on” state switch and greater than 100 °C/W for the “off” state switch [4].

Work on the engine itself has focused on understanding issues controlling the speed of operation, efficiency and power output of the engine. Both experimental and numerical work has shown that the primary factor controlling engine efficiency was the location of the liquid-phase working fluid in relation to where heat was added to the engine. In particular, the use of a wicking structure to draw and hold a thin film of liquid working fluid over the area of heat addition was shown to have a significant impact on engine output and efficiency. Secondary factors controlling engine efficiency were the thermal masses of the two membranes and the compliance of the upper membrane [5].

Recent work in our lab has turned to integrating a thermal switch with the engine to accomplish several goals: (1) to demonstrate engine operation from a continuous heat source, (2) to increase engine operation speed by controlling and increasing heat rejection rates, and (3) to characterize and document the operational characteristics of an engine with heat transfer controlled by a thermal switch.

## 2. EXPERIMENT

The present experimental work was conducted with the apparatus illustrated in Fig. 2. The set-up included a single micro engine and thermal switch. Each engine consisted of a cavity, defined by two silicon die, with square membranes bulk micromachined in them, clamped around a spacer and filled with a two-phase working fluid. Both silicon and silicon nitride membranes were used. Membranes were fabricated via anisotropic wet etching. The top membranes were 6 mm square, and left bare. The bottom membranes, 5

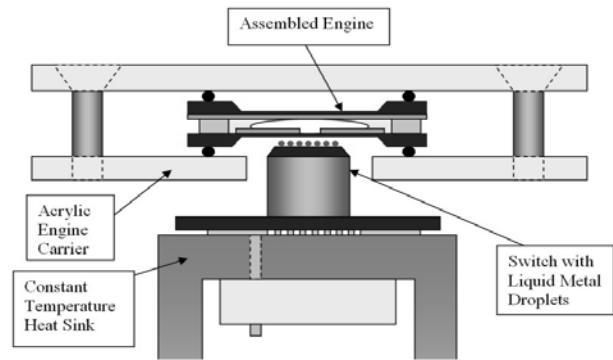


Figure 2. Engine and Thermal Switch

mm square, were further processed. First, a gold thin-film resistance heater was fabricated on the bottom membrane. Then, a capillary wicking structure was fabricated by spinning SU-8 over the heater and defining channels via photolithography. Upon completion, the top die and the bottom die were clamped together, face to face, with 75 micron semiconductor tape between them. The cavity formed between the two membranes was filled with 3M™ PF-5060DL.

The thermal switch below the engine consisted of a liquid-metal droplet array deposited via physical vapor deposition on a silicon die. The micro-droplet arrays were fabricated by preferentially condensing mercury micro-droplets on 30 micron diameter circular gold targets in a 40 by 40 array (1600 targets) on the silicon substrate. The droplet-array die was mounted on a piezo-stack actuator that was able to translate 80 microns at frequencies up to 200 Hz

The engine and thermal switch were assembled as shown in Fig 2. An optical microscope was used to align the micro-droplet array of the thermal switch with the bottom membrane of the engine. The thermal switch was turned “on” by using the stack actuator to move the micro-droplet array up into contact with the bottom membrane of the engine. The thermal switch was turned “off” by using the actuator to pull the micro-droplet array down to create an 80 micron air gap. Heat transfer from a constant temperature heat source or heat sink (located below the switch) to the micro engine could thus be turned on and off at will. Because of experimental limitations only a single thermal switch was used in the present set of experiments. This meant that the thermal switch could be used only for heat addition, or for heat rejection, but not both.

A laser vibrometer was used to measure the deflection of the upper membrane and so determine the

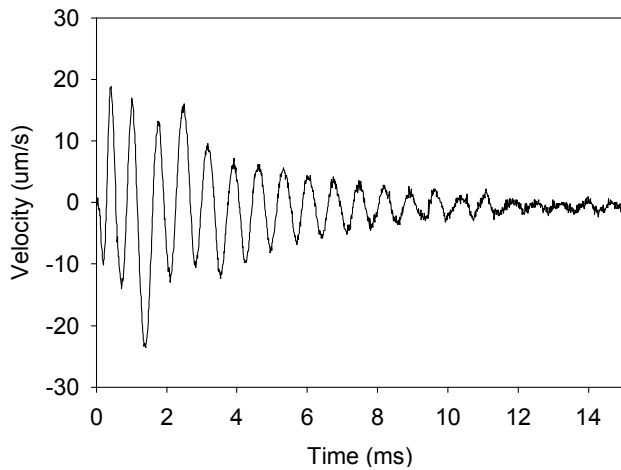


Figure 3. Top Membrane Ringout

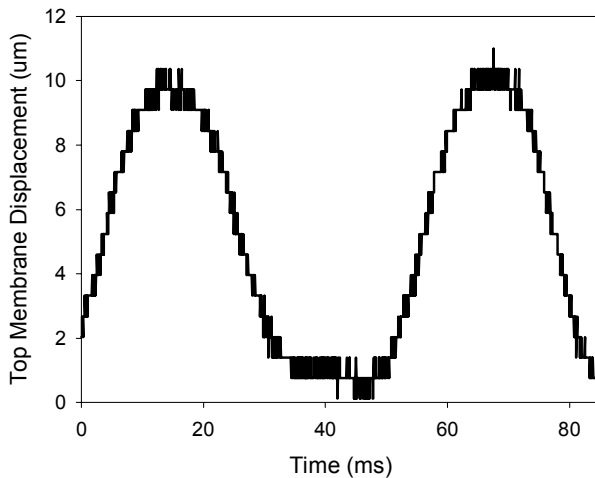


Figure 4. Heat Addition via Thermal Switch

mechanical output of the engine. The thermal switch temperature was monitored with a fine-wire thermocouple inserted just below the micro-droplet array die.

### 3. RESULTS

The internal irreversibility, or losses due to mechanical dissipation, associated with the engine were measured by “ringing out” the engine with a 0.2 millisecond electrical power pulse to the thin-film resistance heater on the bottom membrane. The resulting oscillation of the top membrane, measured by the laser vibrometer is shown in Fig 3. The quality factor or Q of the engine could be extracted from the plot by calculating the decay in kinetic energy of the membrane. In this case, the Q of the engine was found to be 23, for a

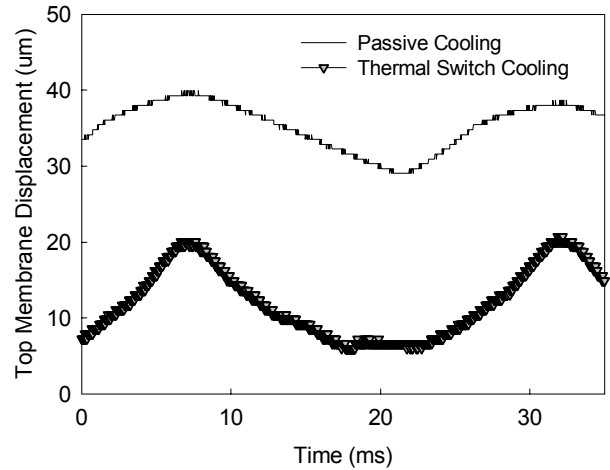


Figure 5. Heat Rejection via Thermal Switch

mechanical loss of 23%. Internal irreversibility, or loss due to viscous dissipation is thus comparable to a macro-scale engine.

The engine was operated from a continuous heat source by employing the thermal switch to control heat addition to the engine. Heat rejection was by passive heat transfer to the ambient. The thermal reservoir was heated to 75 °C and the switch actuated at 20 Hz. The displacement of the top membrane of the engine is shown in Figure 4. Deflection of the membrane is seen to be 8 microns with a mechanical output 15 microwatts.

The engine was operated with the thermal switch controlling heat rejection from the engine. Heat addition was accomplished by pulsing electrical power to the thin-film resistance heater on the bottom membrane of the engine at 40 Hz. The effect of changing from uncontrolled passive cooling to

controlled cooling via thermal switch can be seen in Fig. 5. The displacement of the top membrane of an engine that was actively cooled by the thermal switch is shown with the thick line. For comparison, the displacement of the top membrane of a passively cooled engine is shown with a thin black line. The passively cooled engine produced top membrane deflections of 10 microns. The engine actively cooled by the thermal switch produced top membrane deflections of 13 microns. In addition, the thermal switch maintained both a lower average displacement (because the micro-engine was cooled to a lower average temperature) and more steeply sloped cooling curves (because of a higher heat rejection rate).

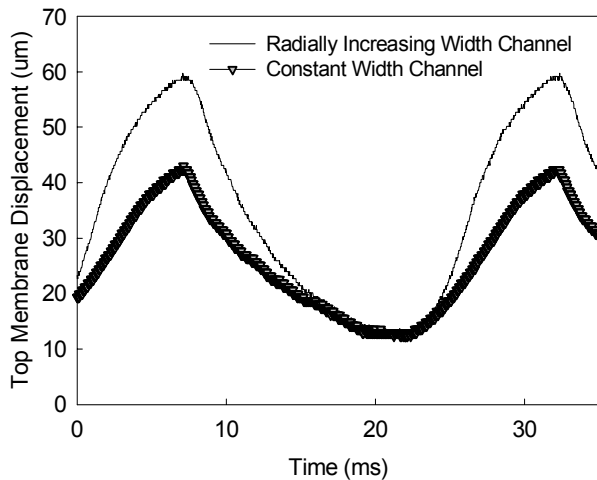


Figure 6. Effect of Wicking Structure and Membrane Material

In Fig. 6, the effect on engine output of the capillary wicking structure and engine membrane material can be seen. Figure 6 shows the displacement of the top membrane of an engine where the top membrane is fabricated from silicon nitride. Switching from the 2 micron thick silicon top membrane, shown in Fig. 5 to the 200 nanometer silicon nitride top membrane in Fig. 6 decreases the thermal mass while increasing the compliance of the membrane. The result is an increase in top membrane deflection (thick line) from 13 to 32 microns. Likewise, changing the capillary wicking structure from one with constant width channels and radially increasing wall thickness to one with radially increasing channel width and constant thickness walls increases both the fraction of evaporator covered by liquid working fluid and the capillary pumping rate. The result (thin line) is a further increase in top membrane deflection from 32 to 50 microns.

The higher heat transfer rates and the greater control over heat rejection enabled by the thermal switch also makes possible higher operating frequencies for the micro-engine. Figure 7 shows top membrane deflection for the engine configuration with a two micron silicon top membrane and constant width capillary channels operating at 100 Hz. Top membrane deflections of 15 microns and a mechanical output of 20 microwatts are obtained at this operating condition.

#### 4. SUMMARY AND CONCLUSIONS

The operation of an external combustion dynamic micro heat engine in which heat transfer to and from the engine has been controlled with a thermal switch has

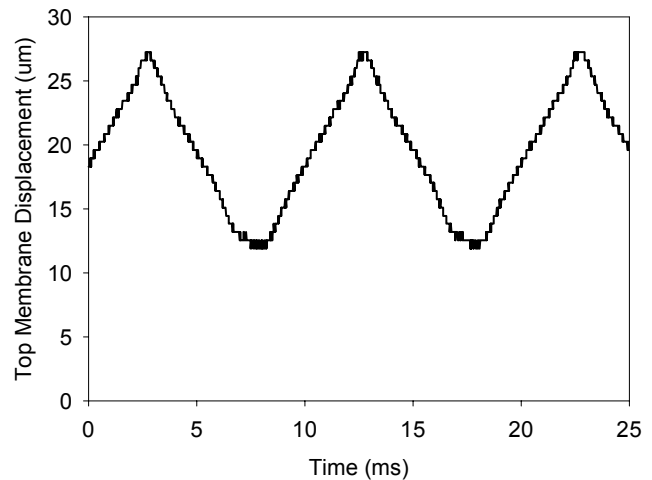


Figure 7. 100Hz Operation using Thermal Switch Heat Rejection

been documented. Use of a thermal switch to control heat addition to the engine enables operation of the engine from a continuous heat source. Use of a thermal switch to control heat rejection from the engine results in increases in both the mechanical output and operating frequency of the engine. Engine cycle speeds up to 100 Hz have been attained. Finally, the internal irreversibility (loss due to mechanical dissipation) of the engine has been shown to be comparable to that in a conventional macro-scale engine.

#### REFERENCES

- [1] A. Mehra, X. Zhang, A.A. Ayon, I.A., Waitz, M.A., Schmidt and C.M. Spadaccini, "A Six-Wafer Combustion System for a Silicon Micro Gas Turbine Engine," *J.MEMS*, Vol.9, No. 4 (2000)
- [2] K. Fu, A. J. Knobloch, F.C. Marinez, D.C. Walther, C. Fernandez-Pello, A.P. Pisano, D. Liepmann, "Design and Fabrication of a Silicon-Based MEMS Rotary Engine," *Proc. ASME IMECE 2001*, Paper No. MEMS-23925, New York (2001).
- [3] C. D. Richards, M. J. Anderson, D. F. Bahr and R. F. Richards, "Efficiency of Energy Conversion for Devices Containing a Piezoelectric Component," *J. Micromech. and Microeng.*, vol. 14, pp.717-721, 2004.
- [4] T. S. Wisler, "Steady State Heat Transfer Characterization of a Liquid-Metal Thermal Switch," MS Thesis, Washington State University, 2005.
- [5] S.A. Whalen, D.F. Bahr, C.D. Richards, and R.F. Richards, "Characterization of a Liquid-Vapor Phase-Change Actuator," *Proc. of ASME IMECE*, Florida, U.S.A., Nov. 5-11, 2005, Paper No. IMECE-82564